Ex 1

ISSN 0332-59

Norwegian Geophysical Society

Geophysica Norvegica

VOL. 32 NO. 2 . 1981
UNIVERSITETSFORLAGET

GEOPHYSICA NORVEGICA . VOL. 32 . NO. 2 . PAGES 15-43 . 1981 UNIVERSITETSFORLAGET

Geophysica Norvegica

is a journal of geophysics, issued under the auspices of the Norwegian Geophysical Society. *Geophysica Norvegica* is mainly intended as a journal for Norwegian authors, but papers from other authors may be accepted provided that the work has been carried out at a Norwegian institution or its content has a special relevance to Norway.

PUBLISHER

Universitetsforlaget: P. O. Box 2959, Tøyen, Oslo 6, Norway
P. O. Box 258, Irvington-on-Hudson, New York 10533

SUBSCRIPTION

Geophysica Norvegica is published at irregular intervals. Order from the Publisher, Universitetsforlaget.

CONTRIBUTIONS

Manuscripts conforming with the rules on page 3 of the cover should be addressed to the editor. The editorial board will appoint referees, who will ensure that the paper meets a sufficiently high scientific standard.

On the latitudinal oscillations of the northeast Atlantic annual mean polar frontal zone

A. MOENE
The Norwegian Meteorological Institute, Oslo

Moene, A. On the latitudinal oscillations of the northeast Atlantic annual mean polar frontal zone. *Geophysica Norvegica*, Vol. 32, No. 2, pp. 15–21. 1981.

An index based on the result of the latitudinal oscillations of the northeast Atlantic annual mean polar frontal zone is introduced. The power spectrum of the index time series is a significant red spectrum at low frequencies with the indication of a spectral peak near a period length of 25–30 years. Due to the resemblance between the given index spectrum and the variance spectrum of the sea surface temperature annual anomalies in the North Atlantic area, the sea surface temperature anomaly is introduced as a climate variability. The power spectrum of the sea surface temperature anomaly coincides with the spectrum of small inertia oscillations caused by the great heat capacity of the oceans. The inertia oscillations are explained by white noise atmospheric forcing.

A. Moene, Norwegian Meteorological Institute, P.O. Box 320 Blindern, Oslo, Norway.

1. INTRODUCTION

The latitudinal oscillations of the northeast Atlantic polar frontal zone have a decisive influence on the weather above Northwest Europe. The oscillations take place on different time scales; daily, monthly, seasonal, and annual latitudinal oscillations can be observed. Greater climate variations observed in Northwest Europe are caused by the oscillations of the annual mean polar frontal zone; this latter type of oscillation will therefore be discussed. The nature of the oscillations is examined for a long period of years. The examination is based partly on daily synoptic charts and on annual mean surface pressure charts as given by Deutscher Wetterdienst (1949–1978). The westerlies appearing in annual mean surface pressure charts are in the mean zone of the polar frontal migrating cyclones, and consequently the westerlies coincide with the annual mean polar frontal zone.

The oscillations of the easterly part of the annual mean polar frontal zone take place between two characteristic locations. The first location is in an easterly direction from the Atlantic towards the continent which is invaded by the mean polar frontal zone between approximately 50 and 60 degrees north.

The second location is in a northeasterly direction from the Atlantic towards the continent, which in this latter case is invaded by the mean polar frontal zone between 60 and 70 degrees north. The significant oscillations of the annual mean easterly part of the polar frontal zone thus take place between the two characteristic locations, and result in significant weather changes in the given areas.

2. INDEX OF THE OSCILLATIONS OF THE ANNUAL POLAR FRONTAL ZONE

Examples of indicators of the oscillations of the annual mean polar frontal zone are given in Fig. 1, which illustrates the deviations from annual normal runoff of two important hydro-electric power-producing rivers in Norway.

The river A, Namsen, is located in central Norway, about 65 degrees north with a precipitation catchment area of about 6000 km² formed mainly by the westerly slope of the mountains. The river B, Glomma, is located in southeast Norway between 59 and 63 degrees north with a precipitation catchment area of about 40,000 km² formed by the east and southeast slope of the mountains.

The annual mean water runoff of the northerly located river Namsen depends on a northerly location of the polar frontal zone; this results in frequent passages of cyclones and a high frequency of winds with west components giving maritime weather conditions with increased amounts of precipitation and air humidity content. Greater than normal runoff of the river Namsen thus depends on a northerly location of the polar frontal zone together with the westerlies. In the case of a northerly location between 60 and 70 degrees north of the polar frontal zone and the westerlies, the north-south orientated mountain chain in South Norway involves a precipitation shadow on the catchment area of the southerly river Glomma. Below normal runoff of the river Glomma is therefore observed in the case of a northerly location of the polar frontal zone. A southerly location, between 50 and 60 degrees north of the annual mean polar frontal zone, results in a higher frequency of easterly and southeasterly components of the surface winds above Norway and above normal precipitation amounts in the catchment areas of the river Glomma. Greater than normal runoff of the river Glomma is therefore observed in the case of a southerly location of the polar frontal zone.

The predominant easterly winds north of the southerly located polar frontal zone result in a dryer continental type of climate in the catchment area of the river Namsen.

In Fig. 1 the cumulative deviations from normal runoff are given by $\sum_{1}^{n}(k-1)$, where $k = \frac{r}{r_m}$, r is annual runoff and r_m is normal runoff (historical mean).

It appears from Fig. 1 that the significant large scale oscillations take place with a phase difference of 180 degrees. This reflects the latitudinal oscillations of the polar frontal zone together with the westerlies. Due to the simultaneous reverse oscillations of the cumulative sum of deviations from normal runoff from the two given rivers, we have thus obtained a numerical index characterizing the latitudinal oscillations of the annual mean polar frontal zone.

3. ON THE SPECTRAL POWER ESTIMATES

The shape of power spectrum estimates provides useful insight into the physical processes of climate variations. A uniform distribution of variance as a function of frequency, white noise, would imply a lack of memory of prior states. A red spectrum in which the variance decreases with increasing frequency implies that some portion of the atmosphere-ocean-cryosphere system remains a memory of prior states, undoubtedly through thermal lag or phase change. Finally, the existence of a pronounced peak in the variance spectrum

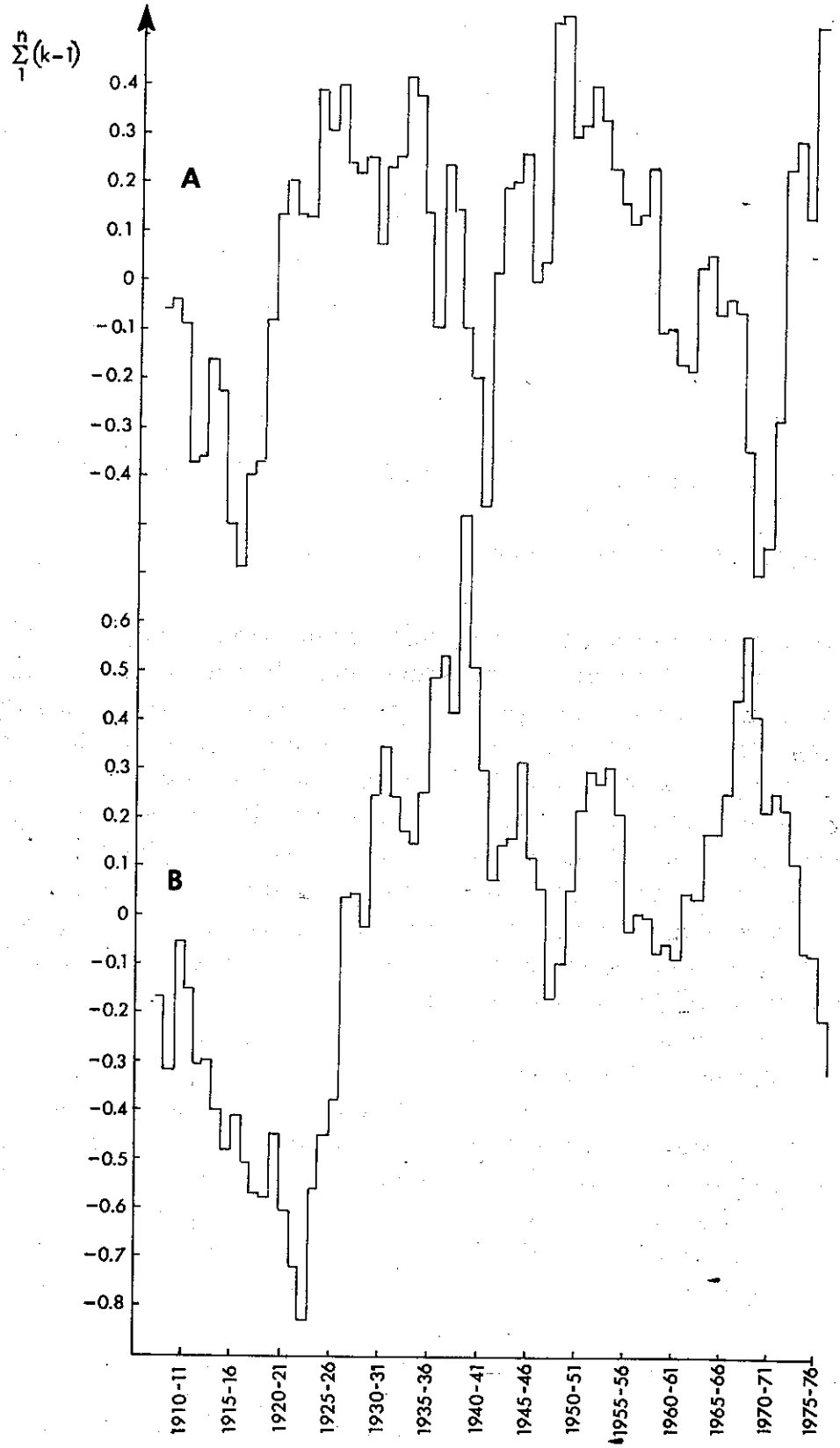

Fig. 1. The cumulative sum of deviations $\sum_1^n (k-1)$ is given, where $k = \frac{r}{r_m}$ r is annual runoff, r_m normal runoff (historical mean). Part A illustrates the sum for river Namsen located in Central Norway with a precipitation maximum in the case of a northerly location of the annual polar frontal zone. Part B illustates the sum for the river Glomma located in southeast Norway with a precipitation maximum in the case of southerly location of the annual polar frontal zone.

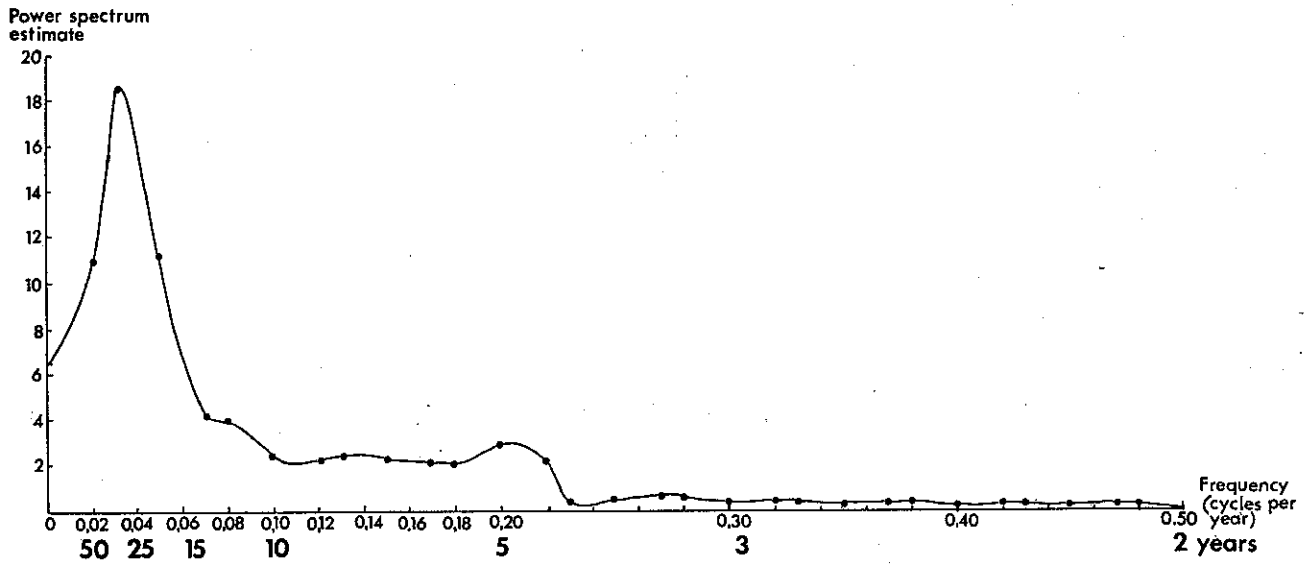

Fig. 2. Power spectrum estimates of the index given in Fig. 1, part A.

would imply some external forcing of the system and/or an internal resonance or interaction mechanism. A computer program calculating the autovariance and power spectrum estimates is applied to the two times series of the cumulative sum of deviations from normal runoff given in Fig. 1. The program, which is given by Dixon (1965) and Jenkins and Watts (1968), also calculates the cross-variance, cross-spectrum, and amplitude and phase of the cross-spectrum. The power spectrum estimates of the time series A is given in Fig. 2.

It may be generally stated from Fig. 2 that the latitudinal oscillations of the annual mean polar frontal zone represented by the time series given in Fig. 1 are characterized by a red power spectrum at low frequencies with a probable spectral peak near a period length of 25–30 years.

4. THEORY

Hasselmann (1976) has introduced a stochastic model of climate variability in which slow changes of climate are explained as the integral response of climate to continuous random excitation by shorter time scale disturbances. Hasselmann and Herterich (1977) have applied this model to a simplified atmospheric and oceanic system. In this system, sea surface temperature (SST) changes are produced by white noise atmospheric forcing. This input is assumed to be balanced by a negative linear feedback representing a power spectrum of SST-anomaly of the form

$$E(\omega) = \frac{A}{\omega^2+\lambda^2} \qquad (1)$$

where ω is the radian frequency, λ is the constant linear feedback factor, and A the constant white noise spectrum.

The E-spectrum given by eq. (1) represents the spectrum of small inertia oscillations about a state of equilibrium. The inertia is ascribed to the great heat capacity of the ocean.

Fig. 3 shows the power spectrum of observed anomaly of the SST of the N Pacific and the belonging power spectrum of the surface atmospheric pressure anomaly, after Davis (1976).

The SST anomaly represents the climate variability, and the surface atmos-

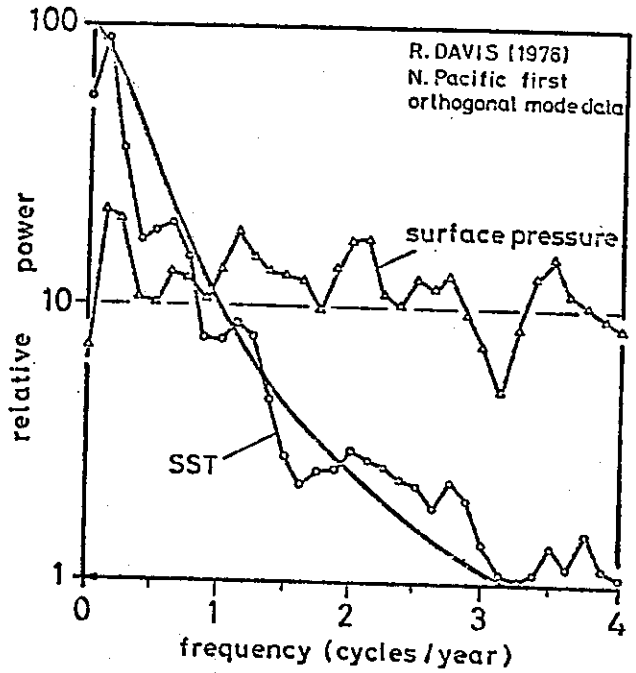

Fig. 3. The power spectra of the anomalies of the SST and the sea surface pressure of the atmosphere. The full curve represents the E-spectrum of the small inertia oscillations caused by the great heat capacity of the Pacific ocean.

pheric pressure the white noise spectrum given in the eq. (1), i. e. the white noise input.

The power spectrum E defined in eq. (1) is also given in Fig. 3, and it appears that the spectra of E and SST nearly coincide. The low frequency oscillations of the SST anomaly may then be regarded as small inertia oscillations due to the great heat capacity of the ocean.

The importance of small inertia oscillations is also evident from the theoretical stochastic models introduced by Lemke (1977). According to Lemke, it is sufficient to represent the ocean by an upper thermal mixing homogenous top-layer in the case of shorter time series. For longer time series, the model, which is based on the principle of energy balance, also includes the deeper layer of the ocean with upwelling. The computed theoretical power spectra which are valid for 55 degrees N latitude of the oceans show the dominating influence of the E-spectrum given by eq. (1) on the SST-spectrum down to frequencies between 10^{-1} and 10^{-2} cycles per year. Lemke introduces into his model a second inertia parameter due to the snowcover, which prevents an increase to infinity of the power estimates at very low frequencies, below 10^{-3} cycles per year.

5. SPECTRAL ANALYSIS OF NORTH ATLANTIC TIME SERIES

J. Bjerknes (1962) has published long time series of annual SST anomalies in the N Atlantic region around the longitude 27.5 degrees W and near to the latitudes 61.5, 57.5, 52.5, 47.5, 42.5, and 37.5 degrees N.

The computed power spectrum estimates of these time series are all red spectra at low frequencies. The spectrum representing 52.5 degrees N is given in Fig. 4 and it appears that this spectrum has a peak near the frequency value of the spectral peak given in Fig. 2. The other SST spectra demonstrate spectral peaks at lower frequencies.

It appears from Fig. 4 that the long time series of the annual anomalies of the sea level atmospheric pressure for the Icelandic area presented by Bjerknes (1962) is characterized by a white noise power spectrum.

In Fig. 4 the inertia E-spectrum is also given by the broken curve representing ω^{-2}, where ω is the radian frequency. It appears that the ω^{-2}-spectrum and the SST-spectrum nearly coincide down to frequencies of about 0.04 cycles per year. Introduction of appropriate values for the constants A and λ in eq. (1) would result in even better fitting of the E-spectrum to the SST-spectrum.

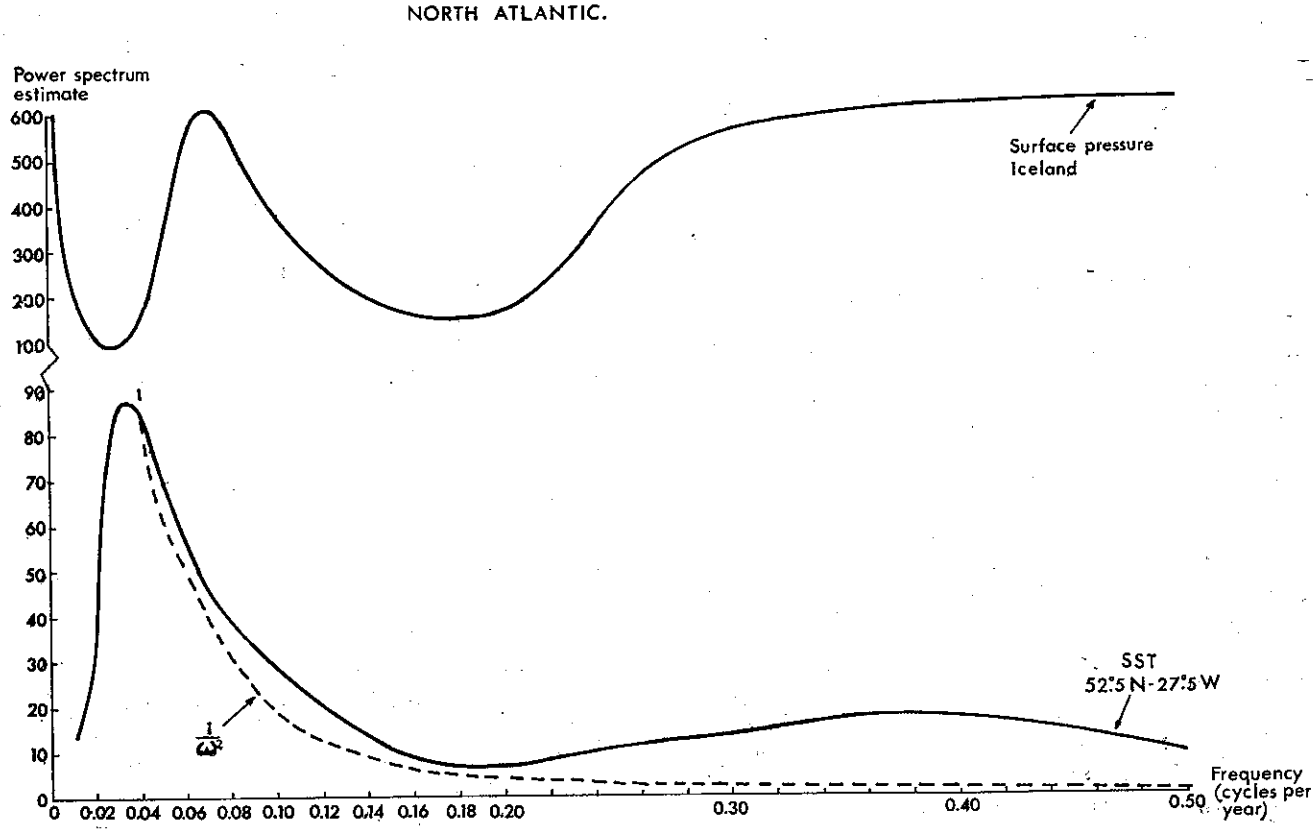

Fig. 4. The power spectra of the anomalies of the SST near to 52.5 degrees N and 27.5 W and the sea surface pressure of the atmosphere in the Icelandic area based on the long time series given by Bjerknes (1962). The unit of the pressure spectral estimates is $(\text{mb.})^2$ per cycle. The inertia E-spectrum is given by the broken curve representing ω^{-2}, where ω is the radian frequency.

6. CONCLUSIONS

Comparisons between the power spectrum of the index given in Fig. 2 and the power spectrum representing the SST anomaly in Fig. 4 show near identical shape of the spectra characterized by a spectral peak approximately at the same frequency corresponding to a period length of 25–30 years. It seems therefore that there are strong reasons for the conclusion that the latitudinal oscillations of the northeast part of the annual mean polar frontal zone are the result of the climate variability represented by the small thermal inertia oscillations caused by the great heat capacity of the Atlantic ocean.

The inertia oscillations can be explained by the white noise atmospheric forcing input.

It also appears by comparison between the long SST anomaly series presented by Bjerknes for 52.5 degrees N and 27.5 W, and the index given in Fig. 1, that a northeast orientation of the annual mean polar frontal zone from the Atlantic towards the European continent between 60 and 70 degrees N implies negative SST anomalies, while an easterly orientation towards the continent between 50 and 60 degrees N implies positive SST anomalies at the given Atlantic ocean area.

REFERENCES

Bjerknes, J. 1962. Synoptic survey of the interaction of sea and atmosphere in the North Atlantic. *Geophysica Norvegica*, Vol. 24, no. 3, p. 115.

Davis, R.E. 1976. Predictability of sea surface temperature and sea level pressure anomalies over the North Pacific ocean. *J. Phys. Oceanogr. 6*, p. 249.

Deutscher Wetterdienst 1949–1978. Die Grosswetterlagen Europas. Offenbach, Germany.

Dixon, W.J. (editor) 1965. Biomedical Computer Programs. Health Sciences Computing Facility, University of California, Los Angeles.

Hasselmann, K. 1976. Stochastic climate models. Part 1. Theory. *Tellus 28*, p. 473.

Hasselmann and Herterich 1977. Klima und Klimavorhersage. Annalen der Meteorologie nr. 12 p. 42. Deutscher Wetterdienst.

Jenkins, G.M and Watts, D. 1968. *Spectral Analysis and Its Applications.* Holder-Day, San Francisco.

Lemke, P. 1977. Stochastische Klimamodelle. Anwendungen auf zonal gemittelte Energiebilanzmodelle. Annalen der Meteorologie nr. 12 p. 47 Deutscher Wetterdienst.

Influence of the interplanetary magnetic field on the earth's magnetic field observed at Ny-Ålesund

SVERRE ALBRIGTSEN, STEINAR BERGER AND ASGEIR BREKKE
The Auroral Observatory, Tromsø, Norway

Albrigtsen, S., Berger, S. and Brekke, A. Influence of the interplanetary magnetic field on the earth's magnetic field observed at Ny-Ålesund, *Geophysica Norvegica*, Vol. 32, No. 2, pp. 23–28. 1981.

Data obtained by groundbased magnetometers at Ny-Ålesund, Svalbard, have been used to investigate the influence of the Interplanetary Magnetic Field (IMF) on the earth's magnetic field for two periods, summer and winter 1974. An effect of the IMF is found in the H-component in summer in the following way: The H-component is more positive in days when the interplanetary magnetic field is directed away from the sun than on days when it is directed towards the sun. Smaller effects occur in the Z- and D-components; in particular the D-component is much reduced in the morning hours between 0600 and 1200 UT when the interplanetary magnetic field is directed away from the sun on disturbed days. During winter time no effects of the IMF can be observed in the magnetic field at Ny-Ålesund. The results are in good agreement with similar results obtained by Friis-Christensen (1971).

S. Albrigtsen, S. Berger and A. Brekke, The Auroral Observatory, University of Tromsø, P.O. Box 953, N-9001 Tromsø, Norway.

From magnetometer observations in Greenland obtained at Godhavn and Thule at about 79.9 and 89.0 degrees geomagnetic latitude respectively, Svalgaard (1968) found that the H-component at Godhavn in the middle of the day was shifted towards lower values during days when the IMF (The Interplanetary Magnetic Field) was directed towards the sun in comparison with the values measured on days when it was directed away from the sun. This was later confirmed by Mansurov (1969). Likewise the Z-component at Thule was found to behave differently on days when the IMF was directed away as compared to days when it was directed towards the sun. These were the first indications that effects of variations in the interplanetary magnetic field can be observed from the ground.

On the maps shown in Fig. 1, the positions of Godhavn (G), Thule (T), and Ny-Ålesund (NÅ) are indicated relative to the auroral oval at 6 different times of day. It is clear from this that Ny-Ålesund stays in the polar cap during a shorter time interval than any of the other two stations. Ny-Ålesund will on the average be inside the polar cap between 15 and 03 UT, and in or slightly south of the auroral oval for the rest of the day.

The relatively mild climate at Svalbard has in modern times made this group of islands an attractive platform for several auroral expeditions. During recent years we have experienced an upswing in this interest. In particular, research has been focused on the behaviour of the polar cap aurora in contrast to the behaviour of the aurora at lower latitudes. It is evident that the geomagnetic field-configuration plays an important part in this differentia-

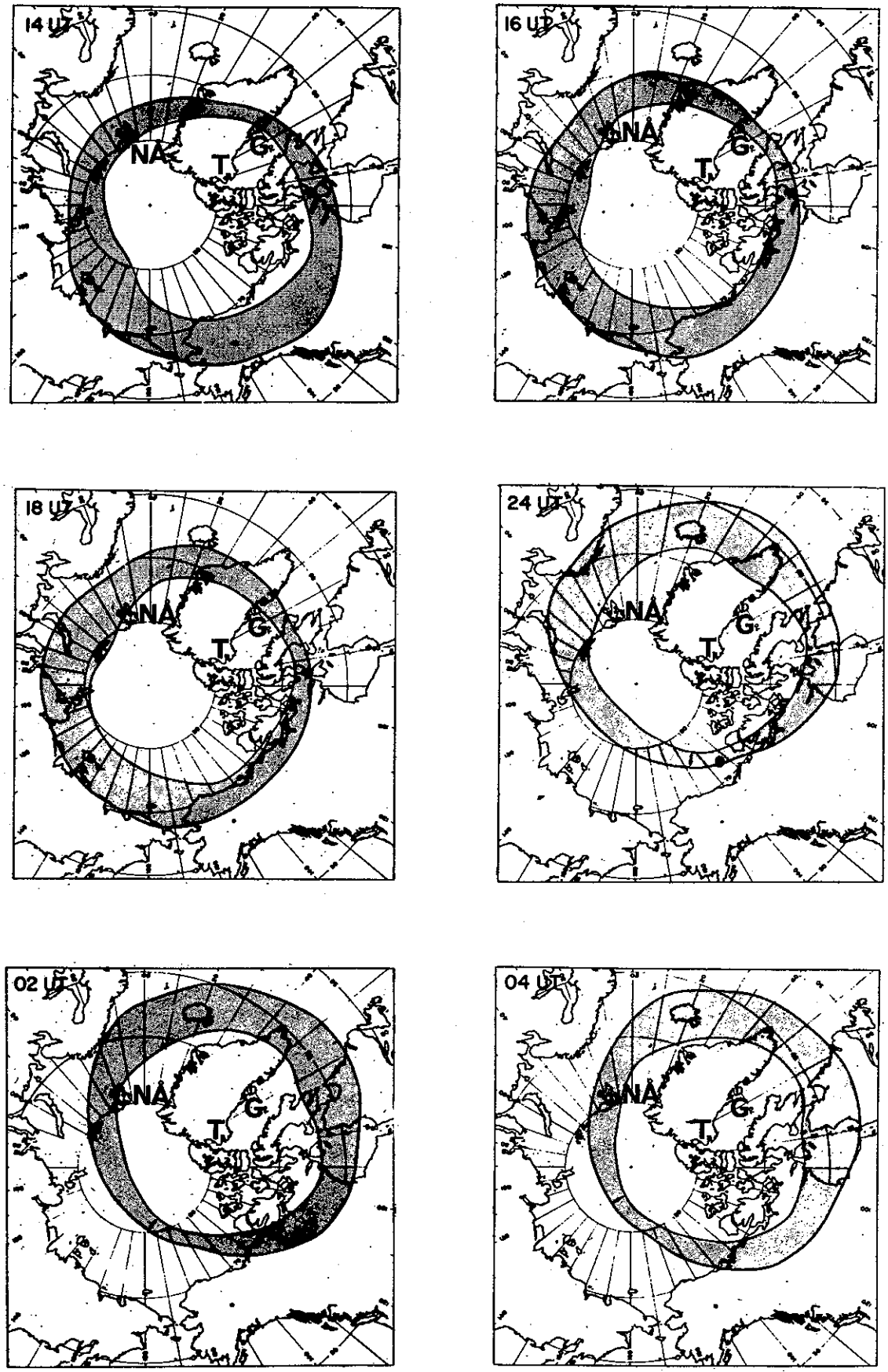

Fig. 1. Maps of the Arctic region where Ny-Ålesund, Godhavn, and Thule are indicated. The position of the auroral oval is also drawn for different times of day. (After Akasofu, 1968.)

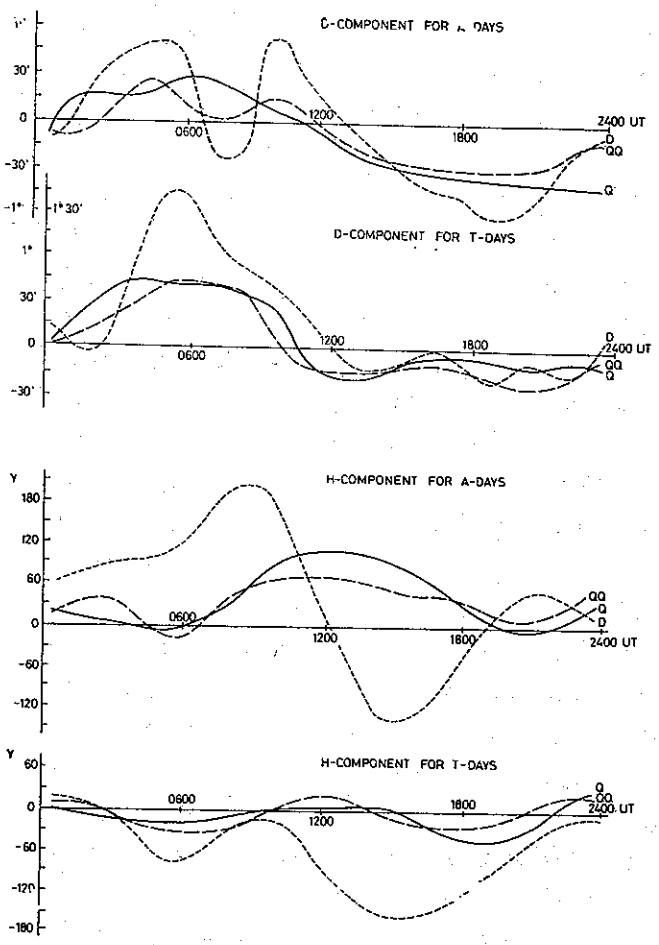

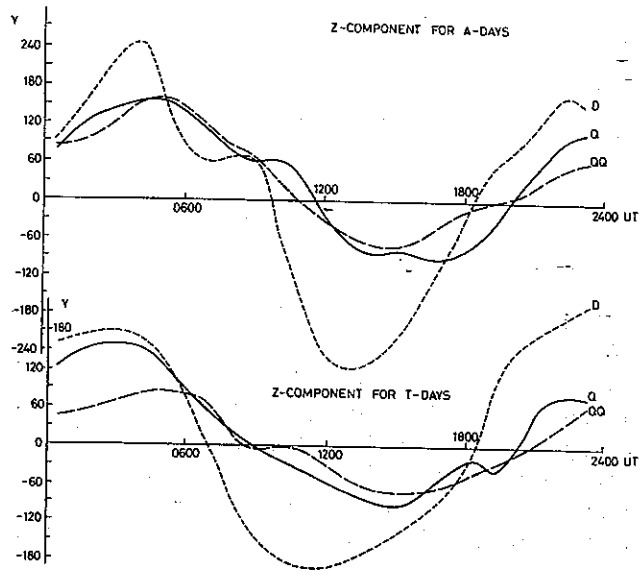

Fig. 2. (a, b, c) Daily mean values for July 1974 of the D, Z, and H components obtained for very quiet (QQ), quiet (Q) and disturbed (D) days in Ny-Ålesund The data are also grouped according to the direction of the interplanetary magnetic field (IMF). A means away from the sun and T towards the sun.

tion. Since this configuration appears to be so strongly related to IMF, it should be of interest to investigate the particular influence by IMF on the geomagnetic field in the Svalbard area.

It is, then, the intention of this report to investigate the possibility of observing these effects from the magnetic field observatory at Ny-Ålesund, Svalbard (75.6 degrees, geomagnetic latitude).

The magnetic observatory in Ny-Ålesund has bee in regular operation since the autumn of 1966, supplying daily variations in the H, D, and Z components of the geomagnetic field. The absolute values of the three components are also obtained on a regular basis. In this work we have chosen data from 1974 to investigate the influence of the interplanetary magnetic field at this latitude. The definition of a quiet day is extremely difficult as irregular variations are almost always present in the magnetometer recordings.

We have chosen, however, to use the quietest days in January, February, and March to establish an average quiet day curve. It is impossible to establish a quiet day during the summer in Ny-Ålesund because the irregular variations are very large even on the most quiescent days; we have therefore used the quiet day mean value obtained from the 3 first months of the year also for summer days.

By the use of this quiet day curve we have derived the hourly mean deviation of all 3 components for all days in January and July 1974.

We have chosen to group the data in several different categories. First of all we have grouped the data according to the

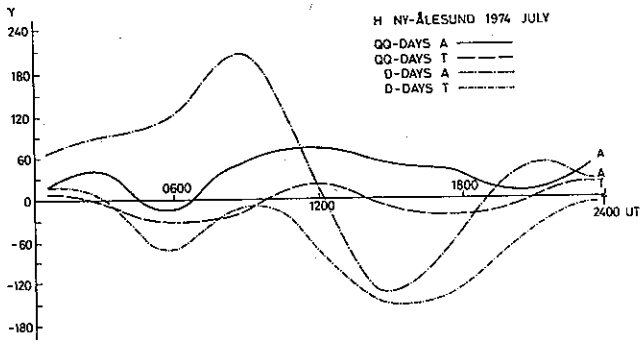

Fig. 3. Daily mean values for July 1974 of the H-component observed in Ny-Ålesund. The data are grouped in disturbed and very quiet days according to the direction of the interplanetary magnetic field. A means away from the sun and T means towards the sun.

polarity of the interplanetary magnetic field as obtained from the World Data Center. Secondly we have grouped the data according to the internationally selected and tabulated very quiet days (QQ-days), quiet days (Q-days), and disturbed days (D-days). Note that the internationally QQ-days are not necessarily the same days chosen as quiet days in this work.

In Figs. 2 a–c we present the hourly mean deviation from the quiet day curve in the D, Z, and H components respectively for July 1974. In the upper panel of each figure the mean values for the QQ, Q, and D days respectively are given on days when the interplanetary magnetic field is directed away from the sun (A-days) and in the bottom panel the corresponding days for the days when the IMF is directed towards the sun (T-days).

There are small differences between the curves for QQ- and Q-days in all three components and irrespective of the direction of IMF. There is a marked difference, however, in the D-component for disturbed days on days when the IMF is directed away from the sun compared to disturbed days on days when the IMF is directed towards the sun. On disturbed T-days the D-component goes through a large eastward deviation of more than one and a half degrees between 0200 and 1200 UT. On disturbed A-days, however, the D-component goes through a full oscillation during this period, the amplitude being about one half of a degree. After midday on disturbed A-days, the D-component oscillates westward, reaching a maximum amplitude of about one degree at about 2000 UT. On disturbed T-days, however, the D-component is also westward between 1200 and 0200 UT but the westward deviation is not significantly different from the behaviour on the other T-days.

There is a significant difference in the behaviour of the H-component on disturbed A- and T-days. On disturbed A-days the H-component goes through a fairly strong diurnal variation, being about 200γ positive at about 0900 UT and about 130γ negative at about 1500 UT. On disturbed T-days the H-component is hardly positive and the oscillation amplitude is about 70γ. The variability in the H-component also appears to be larger on Q- and QQ-days when the IMF is directed away from the sun than on days when it is directed towards the sun.

There are also differences in the Z-component between disturbed A- and T-days, but these are less significant than the differences in the two other components.

In Fig. 3 the daily mean variations in the H-component for July 1974 are shown

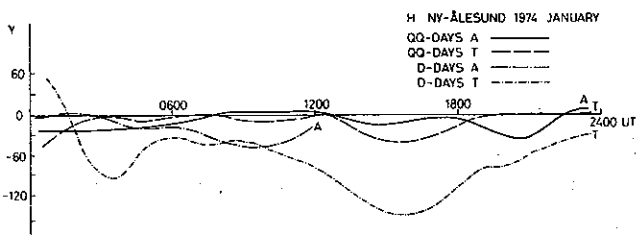

Fig. 4. As for Figure 3 except the time is January 1974.

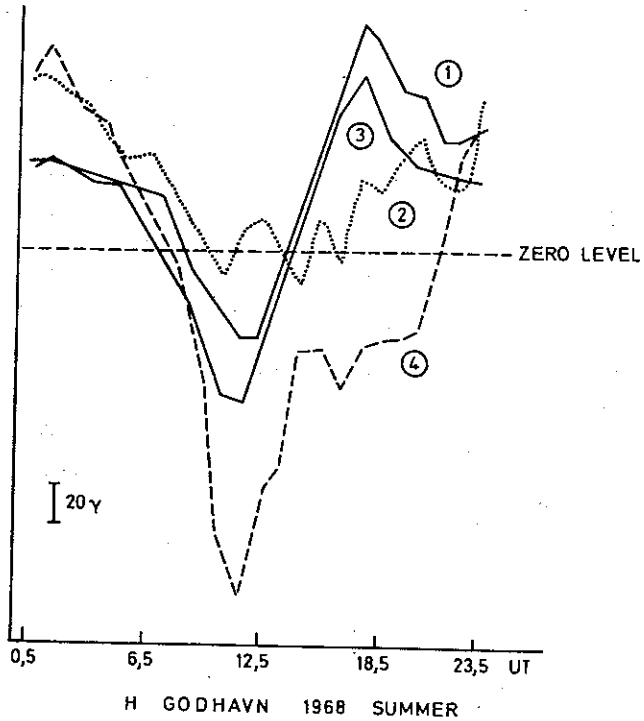

Fig. 5. The daily mean values for July 1968 of the H-component observed at Godhavn by Friis-Christensen (1971). The labels are as follows:
(1) A-sector Q-days
(2) A-sector D-days
(3) T-sector Q-days
(4) T-sector D-days.

for very quiet (QQ) and disturbed (D) days and grouped with respect to the direction of the IMF. Both for very quiet and disturbed days there is a tendency for the H-component to be more positive on days when the IMF is away from the sun compared to days when the IMF is towards the sun.

In Fig. 4 the diurnal mean values of the H-component for January 1974 in DD- and Q-days are shown; these values are grouped with respect to the direction of the IMF. The fluctuations on the January days are, as already mentioned, much less than on the July days, and in particular the variations in the QQ-days are very small. For the D-days there are not enough data to complete the diurnal mean curve, but from the data present between 0000 and 1200 UT on these days there are no significant differences between days when the IMF is directed towards the sun with respect to days when it is directed away from the sun.

CONCLUSION

We have presented data for the mean diurnal variation in the geomagnetic field at Ny-Ålesund which show that the D- and H- component on magnetically disturbed days behave differently in summer on days when the IMF is directed away from the sun than on days when it is directed towards the sun. In particular the H-component before noon on disturbed days is very strongly positively directed when the IMF is directed away from the sun, and is small and mainly negatively directed in the same period for disturbed days when the IMF is directed towards the sun. In winter this difference appears not to be present. One can therefore infer that according to these data the differences in the geomagnetic field configuration due to the IMF will be of little importance to the behaviour of the optical midday aurora at Svalbard.

The H-component in general is also more positive in summer at any time of day when the IMF is directed away from the sun compared to days when it is directed towards the sun, irrespective of whether there are quiet or disturbed conditions.

This result is in full agreement with the results obtained for July 1968 by Friis-Christensen (1971) from Godhavn, Greenland and reproduced here in Fig. 5. In general the H-component at Godhavn is also more positively directed on days when the IMF is directed away from the sun compared to days when it is directed towards the sun.

It is therefore to be concluded that, in summer, effects of the IMF on the geomagnetic field at Ny-Ålesund (76.5° N, invariant latitude) can be observed by groundbased magnetometers. In winter such differences do not appear to be observable.

ACKNOWLEDGEMENTS

We are indebted to Mrs. Liv Larssen and Mr. Petter Brockmann for their assistance in completing this work.

REFERENCES

Friis-Christensen, E. 1971. The influence of the direction of the interplanetary magnetic field on the morphology of geomagnetic variations at high magnetic latitude. *Danish Meteorological Institute R–27.*

Svalgaard, L. 1968. Sector structures of the interplanetary magnetic field and daily variation of the geomagnetic field at high latitudes. *Danish Meteorological Institute, R–6.*

Mansurov, S.M. 1969. New evidence of a relationship between magnetic fields in space and on earth. *Geomag. Aeron. 9,* 622.

Spectral analysis techniques of geophysical data: On the performance of periodogram and maximum entropy method

CHRISTOS I. HALDOUPIS
Institute of Physics, University of Oslo

Haldoupis, C. I. Spectral analysis techniques of geophysical data: On the performance of periodogram and maximum entropy metod. *Geophysica Norvegica*, Vol. 32, No. 2, pp. 29–43, 1981.

Two independent techniques used in spectral analysis of geophysical data, the conventional periodogram and the maximum entropy method (or autoregressive spectral estimator), are applied to synthetic data (harmonic processes plus white noise and autoregressive processes) and to Pi2 micropulsation data, and the results are compared in an attempt to evaluate the method performance and identify any limitations. A number of factors (e.g. noise level, length of data sequence, complexity of spectrum) are considered and their effect on the spectral estimates is investigated. These experiments revealed an inherent difficulty in estimating the proper relative intensities of the spectral components by the maximum entropy technique, even though their location is estimated correctly. In general, the results suggest that there is no strong reason why the maximum entropy method should be preferred to the periodogram, at least for long data sequences.

C. I. Haldoupis, Institute of Physics, University of Oslo, P.O.Box 1048, Blindern, Oslo 3, Norway. Present address: *Physics Department, University of Crete, Iraklion, Crete, Greece.*

1. INTRODUCTION

Spectral analysis of discrete data sequences plays a central role in data analysis and interpretation. Various methods for estimating the power spectrum of a physical data sequence are known and widely used (e.g., see Childers (1978) for an updated collection of reprints). These methods have various but not necessarily the same advantages as well as drawbacks, and therefore must be used with care.

Among the conventional techniques of spectral analysis, the periodogram is quite popular today (partly because of the high computational efficiency of fast Fourier transform (FFT) used for the calculation of the discrete Fourier transform) and has found extensive application, as a standard spectral technique, in computerized Fourier analyser systems used in different fields of research. This technique is believed to give reliable spectra for long data samples of quasi-stationary physical processes. However, there are limitations (e.g. poor frequency resolution) when it comes to analysing short sequences.

In the last ten years several new methods have been developed to estimate spectra with increased frequency resolution. The most successful, the so-called maximum entropy method (MEM), is based on linear prediction filtering, and is equivalent to least-squares fitting of a discrete autoregressive process to the available data.

Since the periodogram and MEM are two completely different methods of spectral analysis, agreement between their

results strongly supports the reliability of the computed estimate. On the other hand, disagreement raises questions about the effectiveness of either method or both. Consequently, testing of these techniques on synthetic data with approximately known spectrum may be particularly useful. Useful conclusions can also be reached by applying both methods on the same data sequence and comparing the resulting estimates.

The purpose of this paper is to present the results of testing the periodogram and maximum entropy analyses on synthetic data (various harmonic processes with additive gaussian noise and autoregressive processes) and on Pi2 micropulsation data, in an attempt to identify advantages and disadvantages, and to point out any inherent limitations which, from the analyst's point of view, may be of considerable importance. Before presenting any results some basic material on both the periodogram and maximum entropy methods follows.

2. THE PERIODOGRAM METHOD

Generally, the periodogram uses the squared magnitude of the discrete Fourier transform (DFT) of the 'windowed' data sequence as a power spectral estimate. If $\{X(t);\ t=0,1,\ldots,N-1;\Delta t\}$ is a discrete physical data sequence (N = number of samples, Δt = sampling interval, $T = N\Delta t$ = period), its power density as a function of frequency (called power density spectrum or power spectrum) is calculated from the equation

$$P(n\Delta f) = |F(n\Delta f)|^2/T = \frac{\Delta t}{N}\Big|\sum_{i=0}^{N-1} X(i\Delta t)\exp(-j2\pi n\Delta f i\Delta t)\Big|^2, \qquad (1)$$

$$n = 0,1,\ldots,(N-1)/2$$

where $\Delta f = 1/T$, and $F(n\Delta f)$ is the DFT which is computed by the FFT algorithm. This representation of the power spectrum is called the 'raw' Fourier periodogram (e.g. see Bringham et al. 1967). In computing the spectrum from Eq. (1) it is assumed that the sampled function $X(t)$ in the interval $(0,T)$ is periodic with period T. This assumption is made whether or not $X(t)$ is actually periodic.

Unfortunately, the spectrum computed by Eq. (1) is not the true spectrum. It can be shown that it is the result of convolution in the frequency domain of the true spectrum and the spectrum of a unit amplitude square pulse equal in length to the period T. This may lead to spurious peaks in the resulting spectrum through 'sidelobe leakage' effects. To reduce leakage we truncate the data sequence by multiplying by an appropriate normalized window function $W(t)$; this is known as 'tapering'. The effect of tapering can also be accomplished by convolution in the frequency domain.

When tapering is applied before computing the DFT (e.g. in the time domain) the resulting spectrum is the 'modified' periodogram, which is not to be confused with, and cannot be obtained as, the result of smoothing the raw periodogram. By truncating the data sequence we get more reliable amplitude information at the expense of less precise frequency resolution. The problem of choosing the best window function is not a trivial one, since requirements of good resolution and spectrum stability must be traded against each other, especially when the length of data is limited (Blackman and Tukey 1958). A general purpose window is defined as

$$W(t) = \begin{cases} \frac{1}{2}\{1 - \cos(2\pi t/T)\}, & 0 \le t \le T \\ 0, & \text{otherwise,} \end{cases} \qquad (2)$$

and is referred to as interval-centred Hanning window.

3. THE MAXIMUM ENTROPY METHOD

Here we shall present briefly some basic features of MEM (for a thorough treatment of the subject see Ulrych and Bishop (1975) and the references cited therein). In MEM, contrary to the conventional techniques, no assumptions are made concerning the data outside the sampled interval. In principle, the MEM provides a procedure by which reliable predictions can be made outside the data interval. This is important, because thereby the length of the record is increased, which in turn leads to a spectral estimate with increased frequency resolution.

The term 'maximum entropy' appeared in the original work by Burg (1967) and is related to the concept of statistical definition of entropy as it is used in information theory. The MEM has been shown (Van den Bos 1971) to be equivalent to computing the spectral estimate from the power spectrum of an autoregressive process (AR), which is fitted to the available data by a least squares method.

The meaning of autoregression is prediction. An AR process is one for which the sample at one time, X_t, is derived from previous values according to the linear equation

$$X_t = a_1X_{t-1} + a_2X_{t-2} + \ldots + a_mX_{t-m} + a_t, \qquad (3)$$

where a_i are constants called the AR coefficients and a_t are samples of a gaussian random process with zero mean and variance σ^2. The number of terms, m, is called the order of the AR process. The power spectrum of an AR process, which has been sampled with a sampling interval Δt, is determined by the equation

$$S(f) = \frac{2\sigma^2\Delta t}{\left|1 - \sum_{i=1}^{m} a_i \exp(-j2\pi fi\Delta t)\right|^2}, \quad f \leq 1/2\Delta t. \qquad (4)$$

Therefore, the power spectrum of a data sequence is calculated by choosing that AR process which best describes the available data.

The procedure of fitting an AR process in the data is often described as the selection of a suitable prediction error filter. Rewriting Eq. (3) as

$$a_t = X_t - a_1X_{t-1} - a_2X_{t-2} - \ldots - a_mX_{t-m}, \qquad (5)$$

means that if the sequence X_t is filtered with an m-point $(a_1, a_2, \ldots, a_m)$ AR filter, the output is the prediction error sequence a_t (a random gaussian variable). In the prediction error filter, which is presented schematically in Figure 1, the predicted value $\hat{X}_t$ is subtracted from the actual input X_t to produce an output error sequence

$$e_t = X_t - \hat{X}_t = X_t - \sum_{i=1}^{m} a_iX_{t-1}, \qquad (6)$$

assumed to be white noise. In practical estimates we compute the error filter coefficients, a_i, and the variance, σ^2, for a chosen filter length m, by minimizing the total squared error $s_m^2 = \sum_{t=1}^{m} e_t^2$ of the filter output. The spectral estimate is then

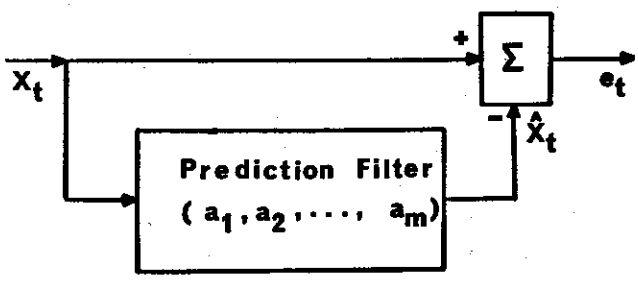

Figure 1. Autoregressive error filter.

computed by using Eq. (4). There are two main approaches for estimating the AR coefficients. The first (Yule-Walker estimates) requires prior computation of the autocovariance function while the second (Burg estimates) does not. For details about these two approaches and a comparison of their results see Ulrych and Bishop (1975).

The above procedure does not lead to a completely unique spectrum because it is necessary to decide what order m of the AR filter should be used. Akaike (1970) introduced a criterion for determining the optimum order m called the final prediction error (FPE). The FPE is composed of two error contributions: the first is due to the unpredictable part of the process (i.e. the noise) and the second due to inaccuracies in estimating the AR coefficients. In general, the first contribution decreases with increasing order m but at the same time the errors in the AR coefficients become larger, tending to increase the FPE. According to Akaike, the appropriate order to be used in the spectral computations is the one for which the FPE is minimum. The FPE is computed from the following equation

$$(\mathrm{FPE})_m = \frac{N + (m + 1)}{N - (m - 1)} P_m, \qquad (7)$$

where N is the number of data points and P_m is the minimum residual sum of squared errors (i.e. the minimum value of s_m^2). The ones in the numerator and denominator must be dropped if the mean has not been removed from the data. Another criterion for optimum order selection proposed by Parzen (1974) leads to similar results as shown by Landers and Lacoss (1976).

The performance of the order selection criteria is not always satisfactory and depends upon the noise present in the data (for example, see Landers and Lacoss 1976). According to Alam (1977), the role of the filter order m has to do with the assumption that the output of the AR filter, e_t, must be white noise, which usually is not true for small m. Ulrych and Bishop (1975) suggest use of the order m that corresponds to the first local minimum of the FPE rather than that for the absolute minimum; they add, however, that this would severely underestimate the required order for more nearly periodic data. In conclusion, it appears that the problem of selecting the appropriate order of the AR process (or the length of the prediction filter) is not yet solved.

4. NUMERICAL RESULTS

In the computations, before performing spectral analysis, a DC-block filter was used to subtract the mean in the data. The interval-centred Hanning window (e.g. Eq. (2)) was applied in the periodogram (or FFT) method to eliminate sharp discontinuities at the ends of the time record in order to reduce leakage effects in the spectrum. The MEM subroutine used to compute the AR coefficients was based on the recursive procedure by Andersen (1974). The noise used in the generation of synthetic data sequences was produced by means of using an algorithm given by Otnes and Enochson (1978).

Synthetic data. The periodogram and ME techniques were used to compute the spectra of various discrete time sequences produced by the superposition of sinusoids and gaussian noise. First we present a simple case. Figure 2a shows normalized power spectra related to a relatively long sequence (by 'long' we mean that the signal period is quite a few times less than

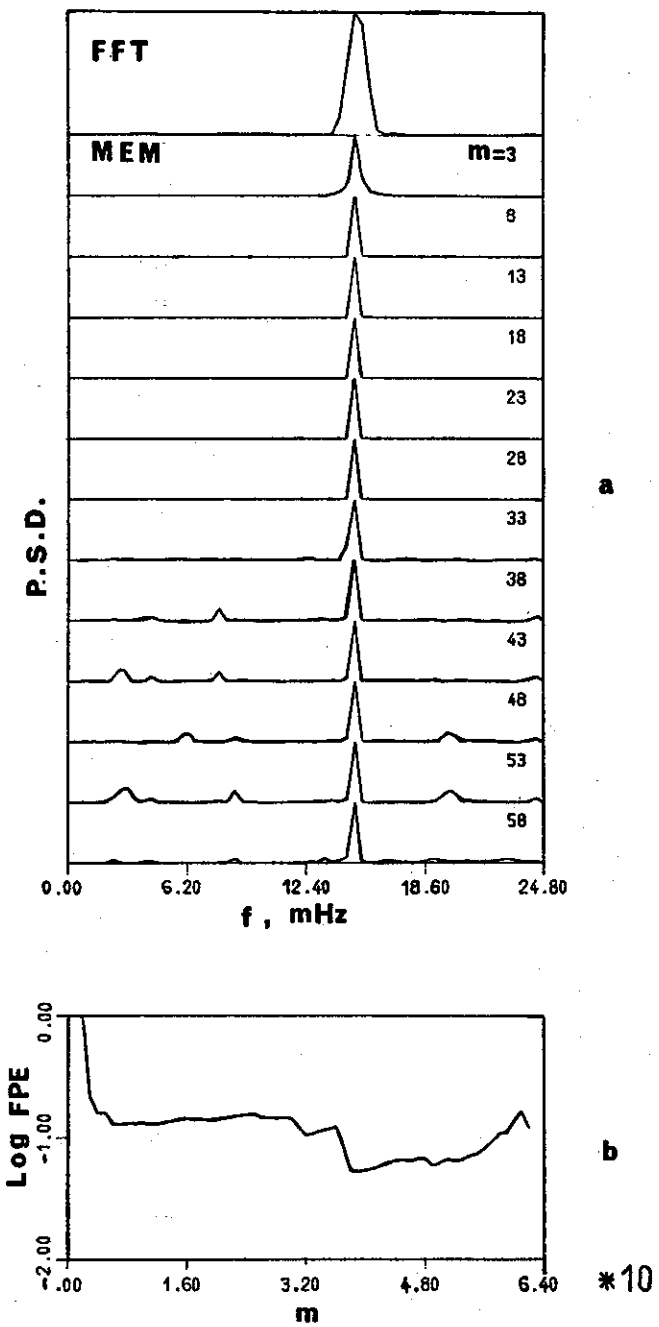

Figure 2. Periodogram and MEM power spectra of a 64-point time sequence sampled from Eq. (8). Figure 2b shows the associated FPE criterion as a function of the order m of the AR process.

the length of the sequence) of a sine wave plus noise

$$X_i = 100 \cos(2\pi \text{ fi } \Delta t + \varphi) + n_i, \quad i = 1,2,\ldots, N, \tag{8}$$

where the sampling interval Δt was set equal to 20 s (Nyquist frequency is 25 mHz), f = 15 mHz, $\varphi = 0°$ and signal-to-noise ratio (SNR) 18 dB. The first top spectrum is computed by means of the FFT (periodogram) method. The position of the sinewave frequency is accurate, but the peak is broad chiefly because of the limited length of the data sample. The rest of the spectra are computed by MEM for different AR orders m shown in the upper right corner of each figure. It is interesting to see that the MEM spectral estimate remains stable for a wide range of orders. The variation of the FPE criterion with m is shown in Figure 2b. Notice that the spectrum for m = 38, at which the FPE has its minimum (according to the theory, this is the optimum AR order), has some small spurious peaks.

Generally, from experiments with harmonic processes plus noise, it has been found that there is spurious detail appearing in the spectrum after a certain order m which depends upon the noise level, the phase of the harmonics and the complexity of the spectrum. For simple harmonic processes and moderate noise levels (less than about 50%), this critical order occurs at about half the number of points. This result agrees with the suggestion made by Ulrych and Bishop (1975) that a cutoff of approximately m = N/2 must be imposed when the FPE is estimated using the Burg method. The same authors have also suggested using in the spectral computations that order m at which the first local FPE minimum takes place. Our results suggest that this is not really necessary, because almost always the spectrum remains fairly stable for quite a few orders higher than the first minimum of the FPE curve.

Next we consider a relatively short data sequence. For such short sequence the

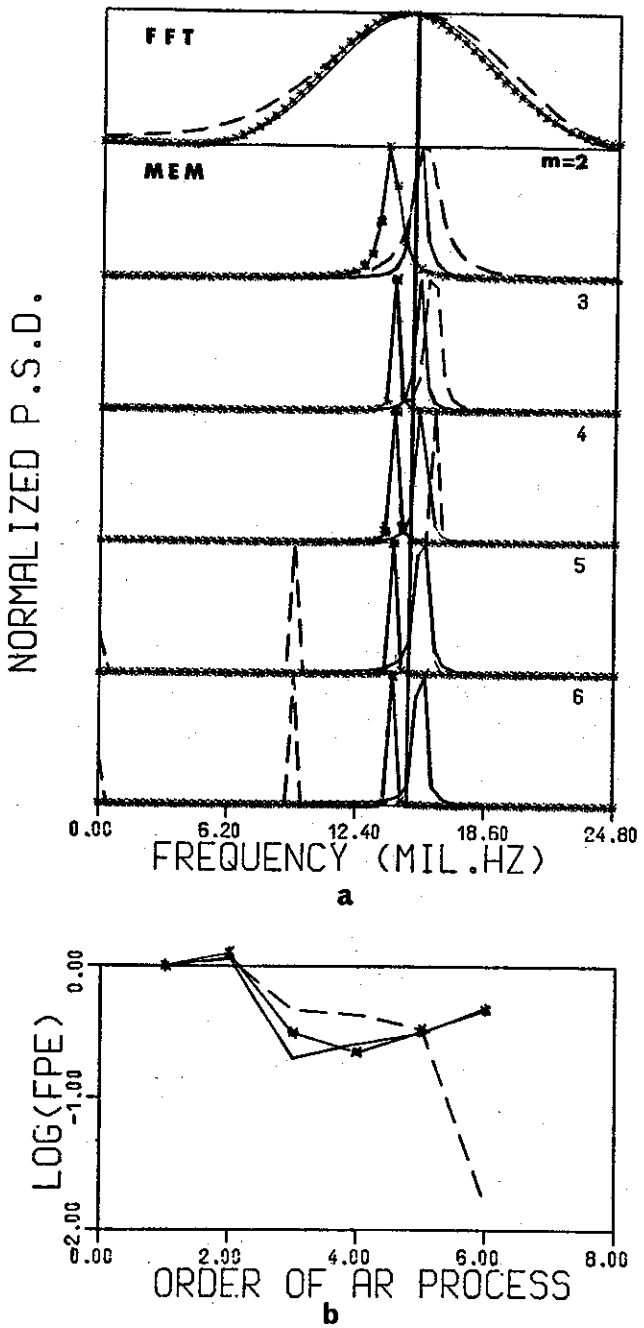

Figure 3. Figure 3a shows the periodograms and MEM spectral estimates of a short 8-point sequence sampled from Eq (8) for three different initial phases φ. The solid line spectra correspond to $\varphi = 0°$, the *-solid ones to $\varphi = 60°$, and the dashed-line spectra to $\varphi = 160°$. The effect of the initial phase on the FPE is shown in Figure 3b.

MEM can provide a better estimate, in terms of frequency resolution, compared to the broad periodogram; however, the position of the spectral peak may be somewhat uncertain depending upon the initial phase of the sinusoid.

The spectra in Figure 3a correspond to an 8-point data sequence sampled from Eq. (8) for the same frequency and SNR as before. In Figure 3a there are three different sets of spectra, corresponding to three initial phases φ, superimposed for comparison. The perpendicular solid line at 15 mHz indicates the position of the sinewave frequency. Inspection of this figure shows: 1) the MEM estimate is superior in frequency resolution compared to periodogram, 2) the MEM spectra are subject to peak-shifting depending upon the initial phase, 3) the shift in frequency differs for different orders m. It should also be mentioned that no 'line-splitting' (e.g., see Fougere 1977) was observed for the moderate noise levels used here.

Similar tests on longer sequences suggest that the effect of the initial phase on the location of the spectral peak is less important. Chen and Stegen (1974) have found, by varying the initial phase continuously from 0 to 360°, that the frequency shift follows a sinusoidal variation whose amplitude decreases with increasing sample length. The initial phase has also an effect on the FPE as shown in Figure 3b.

For more complex harmonic processes it was found that the estimation of the correct spectrum using MEM involves some degree of difficulty. The main problem is not in the accurate location of the position of the spectral peaks but in the estimation of the correct intensities of the peaks. On the other hand, the FFT method provides reliable estimates for long sequences while for short ones the main drawback is the poor frequency resolution. It was found that for relatively long data sequences the MEM locates the peak position quite accurately (error less

than 5%) when the order of the AR process is in the range from about N/5 to 2N/5 where the first FPE minimum almost always occurs. This range expands towards higher orders for lower noise levels and shorter data samples. When $m \simeq N/5$ the resulting estimate is usually broad and/or resolves some of the existing peaks. For higher orders (especially when $m > N/2$) there is peak-shifting, and spurious detail occurs in the spectrum; this effect is accentuated at higher noise levels.

To illustrate some of the above results we present a limited number of examples here. The next two figures correspond to two different sequences sampled from the following harmonic process plus noise

$$X_i = 100\cos(2\pi f_1 i\Delta t + \varphi) + 50\cos(2\pi f_2 i\Delta t) + n_i,\ i = 1,2,\ldots,N. \quad (9)$$

Figure 4a shows spectral estimates for $\varphi = 60°$ and 30% noise level (the noise level is defined as the ratio of rms value of noise to rms value of signal). The first spectrum from top is the periodogram, which has two relatively broad peaks centred at 15 and 5 mHz with relative power ratio of about 4 to 1. The dashed lines in the same figure indicate the position and relative intensities of the two spectral lines in accordance with Eq. (9). The rest of the spectra are MEM estimates for different orders shown in the upper right corner of each figure. Notice that use of a low order does not expose both spectral peaks (e.g. m = 4). On the other hand, when m is in the range from about 10 to 25, the peaks are located accurately (e.g. see spectra for m = 13, 22) but their relative intensities are in error. When m > 25 there is peak-shifting and spurious peaks appear in the spectrum. The FPE, shown in Figure 4b, has its first minimum at m = 13 and its absolute minimum at

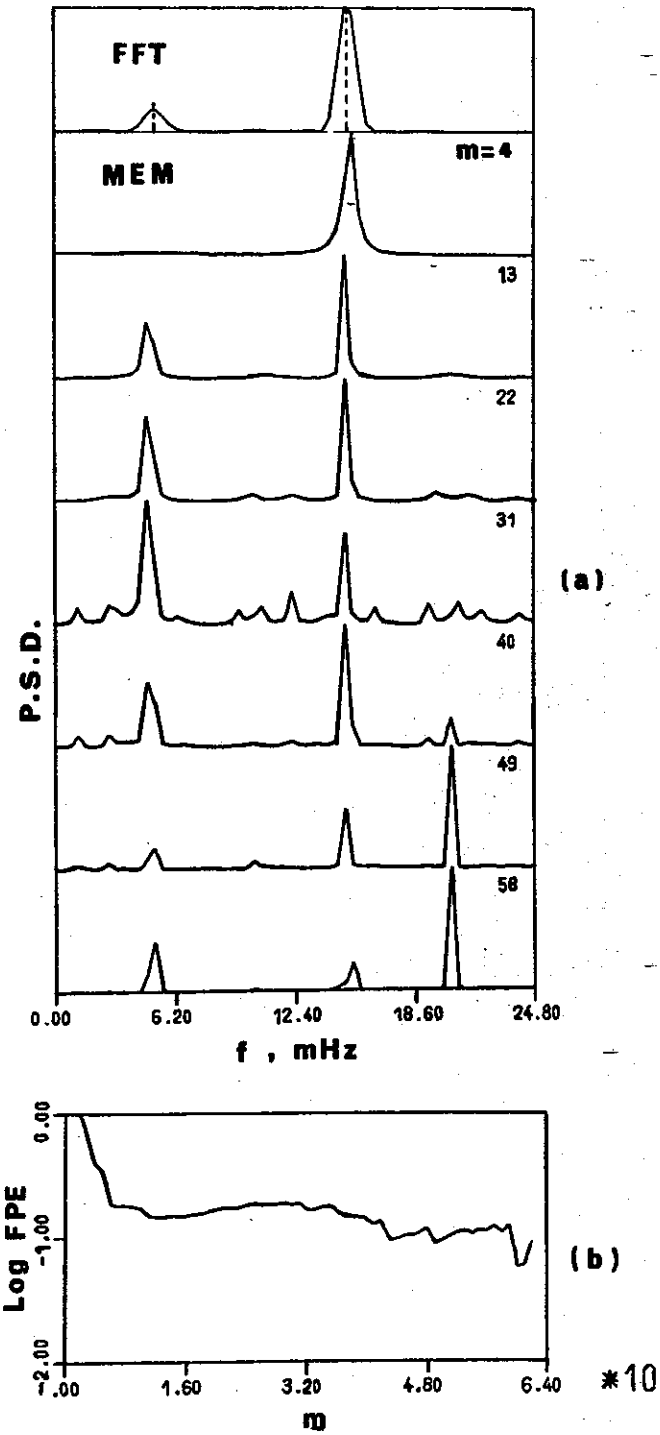

Figure 4. Figure 4a shows FFT and MEM spectra of a 64-point (T = 1280 s) sequence of 2 sine-waves plus noise sampled from Eq. (9). The relative phase is $\varphi = 60°$. The FPE criterion as a function of order m is shown in Figure 4b.

m = 58; the spectrum computed for the last order (shown in Figure 4a) is unrealistic. The results of experiments with harmonics plus noise suggest that, in

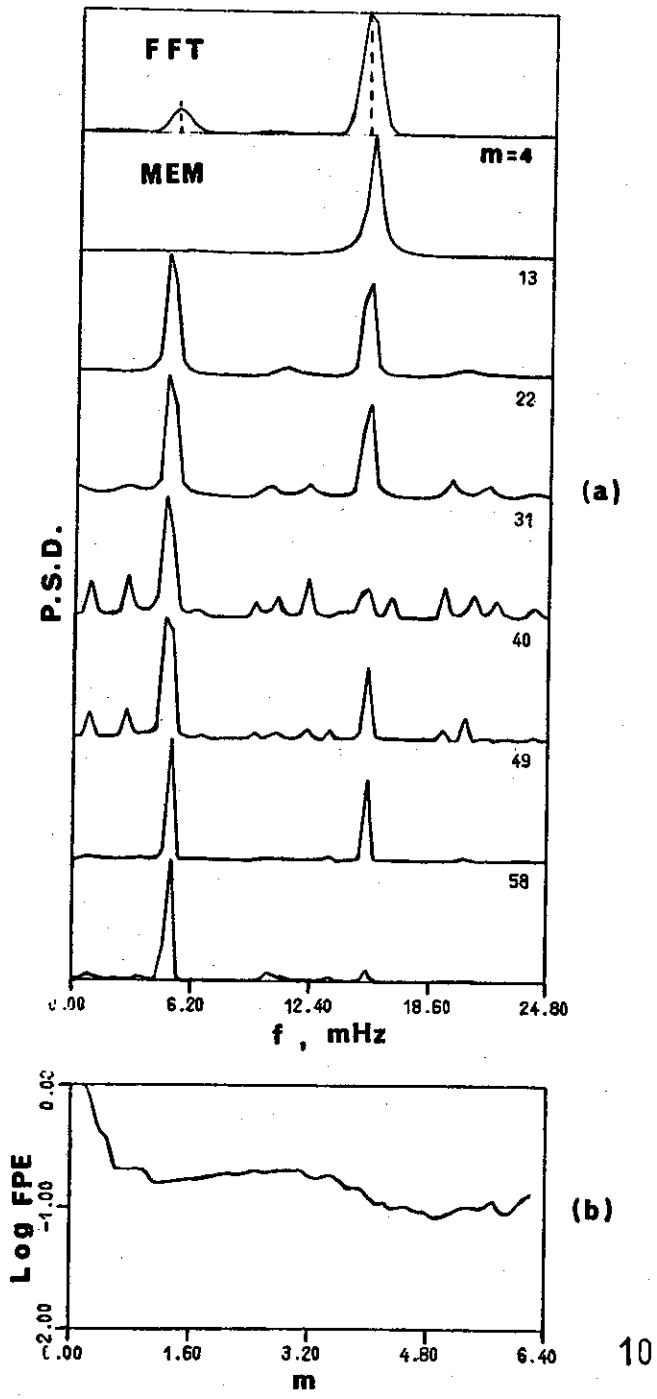

Figure 5. This figure should be compared with Figure 4. The purpose is to show the effect of the relative phase of the harmonics on the corresponding spectra. Here again the time sequence is sampled from Eq. (9) with all the parameters kept the same as in Figure 4 except for the relative phase; here $\varphi = 160°$.

general, the FPE exhibits a sudden decrease up to a first local minimum and then increases gradually up to an order where it starts fluctuating; the absolute minimum occurs almost always at a higher order. The results show that the MEM estimate remains fairly stable (especially the location of the peaks) for the values of m corresponding to the gradually and smoothly increasing portion of FPE-curve. This suggests that a more stable spectrum could be obtained by averaging various estimates computed for different m ranging from N/5 to 2N/5.

Figure 5 depicts a similar situation as Figure 4, where all parameters are kept the same except for the relative phase, which has changed to $\varphi = 160°$. Comparison of the two figures shows that: 1) there is no significant change in the periodogram, 2) there are some minor changes in the detailed form of the FPE-curve, but the order where the first minimum occurs remains the same and 3) the change in phase has introduced a considerable degree of variability in the MEM spectral estimates, especially on the relative peak intensities.

The examples that follow are from a more complicated harmonic process, which is comprised of an amplitude modulated wave, a sinewave and additive noise, defined by the equation

$$X_i = 60(1 + \cos(2\pi f_m i\Delta t))\cos(2\pi f_c i\Delta t) + 50\cos(2\pi f_1 i\Delta t + \varphi) + n_i,$$
$$i = 1,2,\ldots,N. \qquad (10)$$

A number of MEM spectra are shown in Figure 6, corresponding to data sequences sampled from Eq. (10) for $\Delta t = 20$ s, $f_c = 8$ mHz, $f_m = 4$ mHz, and $f_1 = 18$ mHz. Comparison of every spectrum in Figure 6 with the known one (first from top) shows good agreement with respect to the peak location and spectral width, but the relative intensities are in error. Figure 6a illustrates the effect of the relative phase of the harmonics on the

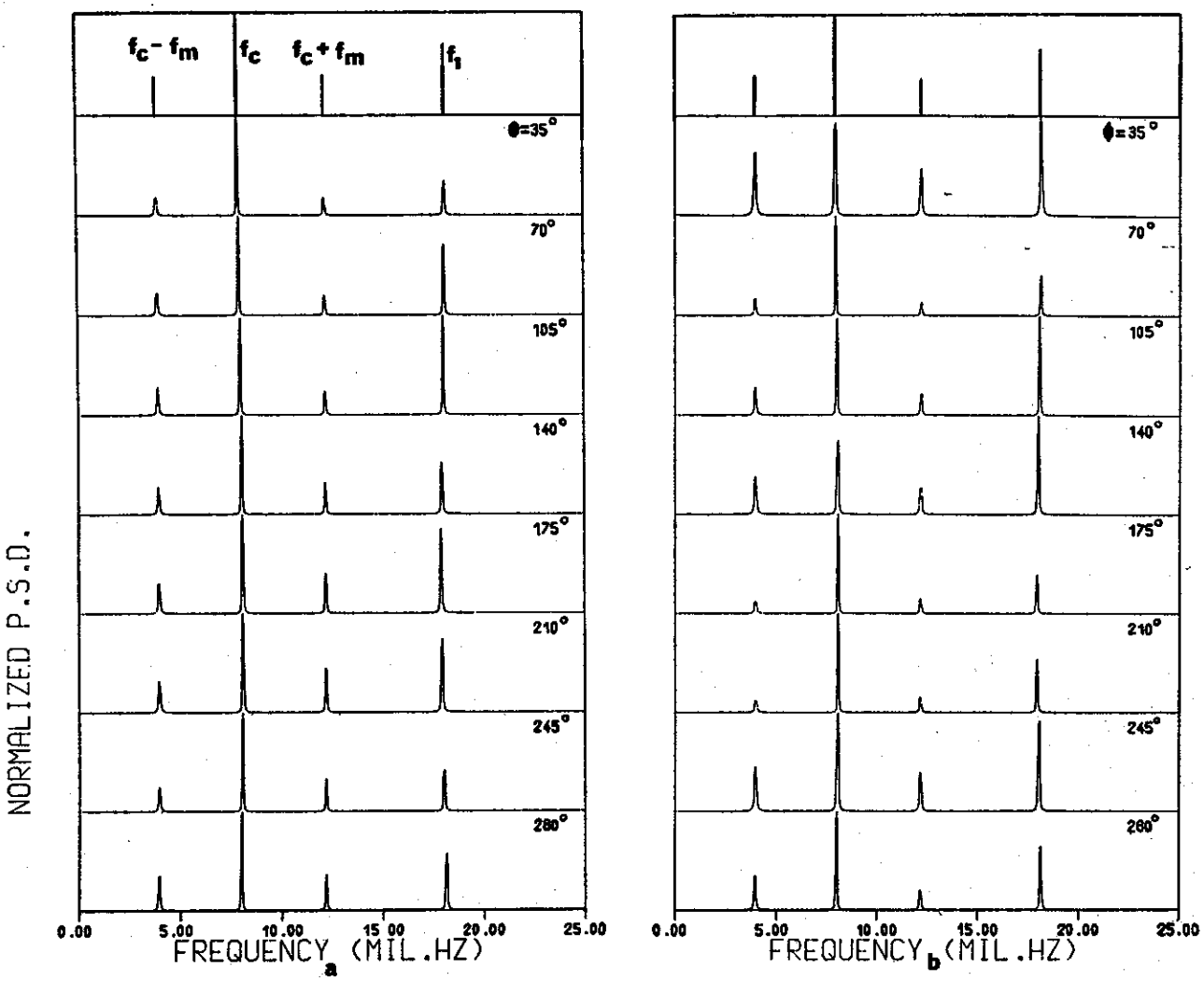

Figure 6. MEM spectra for various 64-point sequences sampled from Eq. (10) for different relative phases φ. The only difference between Figure 6a and 6b is in the noise level. Notice that there is an effect of φ and noise level on the spectra (especially on the peak intensities).

computed spectra. These spectra correspond to time sequences generated from Eq. (10) for different phase φ (shown in the upper right corner) but for the same noise level ($\simeq$ 13%). Figure 6b depicts a similar situation as Figure 6a but the noise level is higher ($\simeq$ 18%). Comparison of these figures shows clearly that for the case of harmonic processes plus moderate noise levels, the MEM estimate could depend on both the noise level and the phase of the harmonics. The main effect of these two factors appears to be on the relative peak amplitudes rather than on the peak location. It should be mentioned that for the computation of MEM spectra shown in Figure 6 we used the order suggested by the first FPE minimum.

From experiments with short data sequences it was found that the MEM gives superior frequency resolution and locates the peaks accurately only if the data sample is sufficiently long. The problem is particularly acute when analysing waveforms with relatively complex spectrum. It has been found that if the sequence is shorter than a critical length, the MEM

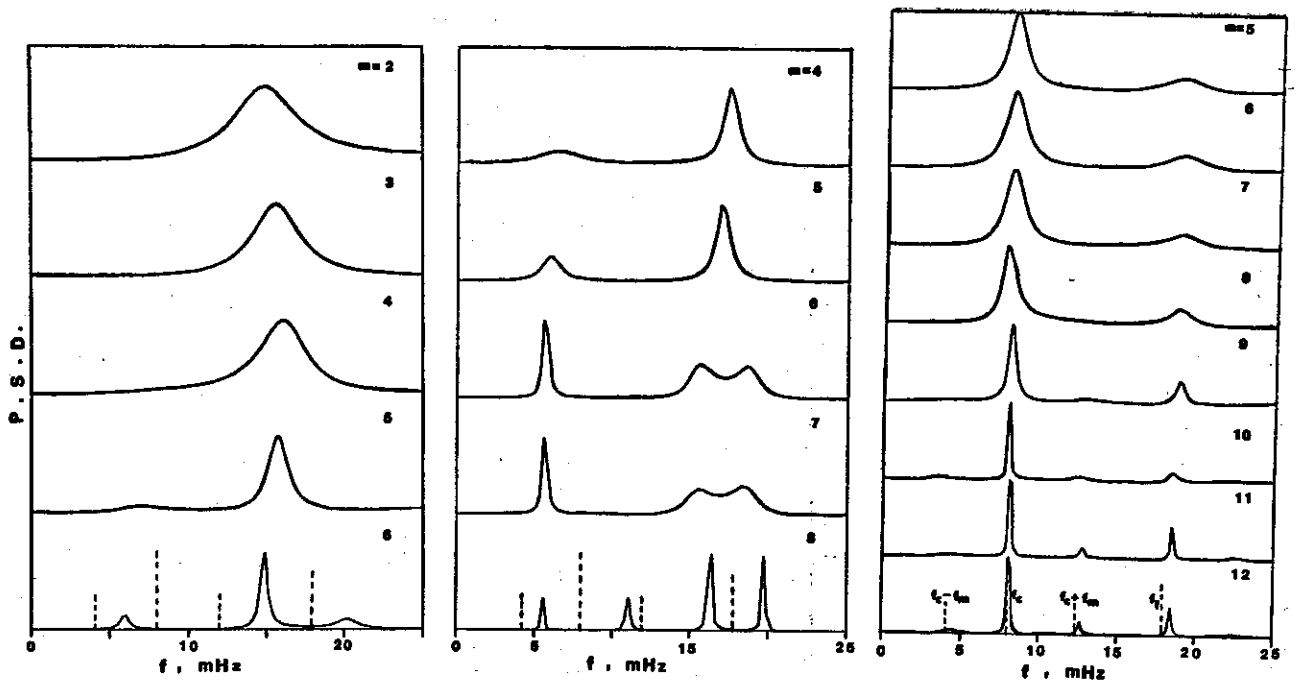

Figure 7. Results of MEM spectral analysis for short data sequences suggest that, especially for waveforms with complex spectrum, the length of sequence has an effect on the resulting spectum. All spectra correspond to time sequences sampled from Eq. (10) for the same phase ($\varphi = 30°$) and noise level (12%). Figure 7a, 7b, and 7c correspond to 8-, 10-, and 16-point sequences respectively. The dotted lines indicate the true spectrum.

gives unreliable estimates. Since the result depends on various factors (e.g. noise level, phase of harmonics) in a rather unpredictable manner, it is difficult to decide what is the critical minimum data length required for analysis; experience shows that it depends also on the complexity of the waveform.

Chen and Stegen (1974) have shown that the length of a data sample causes shifts in the peak location which gradually decline as the sequence length increases; their experiments were based on the simplified model of a sinusoid plus noise. Our results suggest that for more complex harmonic processes, the errors introduced in the spectrum are more serious and affect all the spectral characteristics (position, amplitude, spectral width) of each peak to a different extent. In addition to the above conclusions it was found that the number of terms of the filter (i.e. the order m) has a great influence on the quality of the spectrum. While for long sequences the most appropriate order m (usually suggested by the first FPE minimum) lies well below N/2, for short sequences it is usually above N/2 (for short sequences when using $m < N/2$ the resulting estimate is rather broad, having poor frequency resolution). To illustrate some of the above conclusions, we present Figure 7 which shows MEM spectra for various orders m corresponding to three different, relatively short, data lengths sampled from the same harmonic process given by Eq. (10).

Testing of the performance of both methods has also been carried out on synthetic data generated from AR processes. Details are discussed in a report by Haldoupis (1980). Here some of the results are presented in brief. For short data samples of AR processes, the MEM esti-

mate is more reliable as compared to the broad periodogram, but some degree of ambiguity exists due to uncertainty in choosing the appropriate order m. The FPE criterion is of limited usefulness because in most cases the FPE curve decreases monotonically. Experience shows that for short sequences at least an order m = N/2 should be used. From experiments with long AR sequences, it was found that both methods locate the peak position accurately but that the relative peak intensities differ. The appropriate order m is approximately confined in the range from that m where the first FPE minimum occurs to about m = N/3. The periodogram was found to have considerable structure while the MEM estimate computed for various orders is always smoothed.

Micropulsation data. In the case of real data (here Pi2 pulsation data are used), we do not know the true spectrum in order to test the computed spectra. However, it is worth comparing the FFT and MEM estimates since they are computed using two different techniques, so that agreement constitutes strong evidence that they represent the true spectrum (this comparison, of course, makes more sense for long sequences for which both techniques provide comparable resolution). Another factor, especially useful when we deal with short sequences, is the stability of the MEM spectra for different AR orders m; according to experiments with synthetic data, a stable MEM spectrum is most likely the true spectral estimate.

First we considered a large number of relatively long sequences of Pi2 data and computed MEM spectra for different orders m. In most of the cases the FPE curve exhibits a well-defined minimum for an order m ranging from N/10 to N/5. The spectrum computed for the order suggested by the FPE minimum is a rather broad smoothed spectrum. The results suggest that the most appropriate order that can be used in spectral computations is in the range from N/5 to N/3. For these orders, the computed spectra exhibit better frequency resolution than the one corresponding to the FPE minimum, and show little variation with respect to their spectral characteristics. On the other hand, when m is greater than N/3 various peaks appear in a random manner in the spectrum and spectra for successive orders have significant differences. The degree of agreement between the FFT and MEM estimates is poor and varies for different data samples. Usually, there is only a general resemblance but the spectra differ considerably in detail. The differences are more serious for the relative intensities and widths of the spectral peaks and less important for the location of the peaks. Also it is true to say that in general the MEM estimates are smoothed as compared to the more structured periodograms.

Some of the above conclusions are illustrated in Figure 8 where the FFT and various MEM spectra are shown for 4 different Pi2 pulsation sequences. Notice the poor agreement between the FFT and MEM estimates especially in Figures 8a and 8c. The ME spectrum corresponding to the order suggested by the FPE minimum (shown only for the three cases) is rather broad and smoothed as compared to the FFT spectrum. Inspection of these figures shows that there is always a difficulty in choosing the correct order AR process that fits the data.

Contrary to long sequences, the MEM results are promising when this method is applied on short time sequences. The

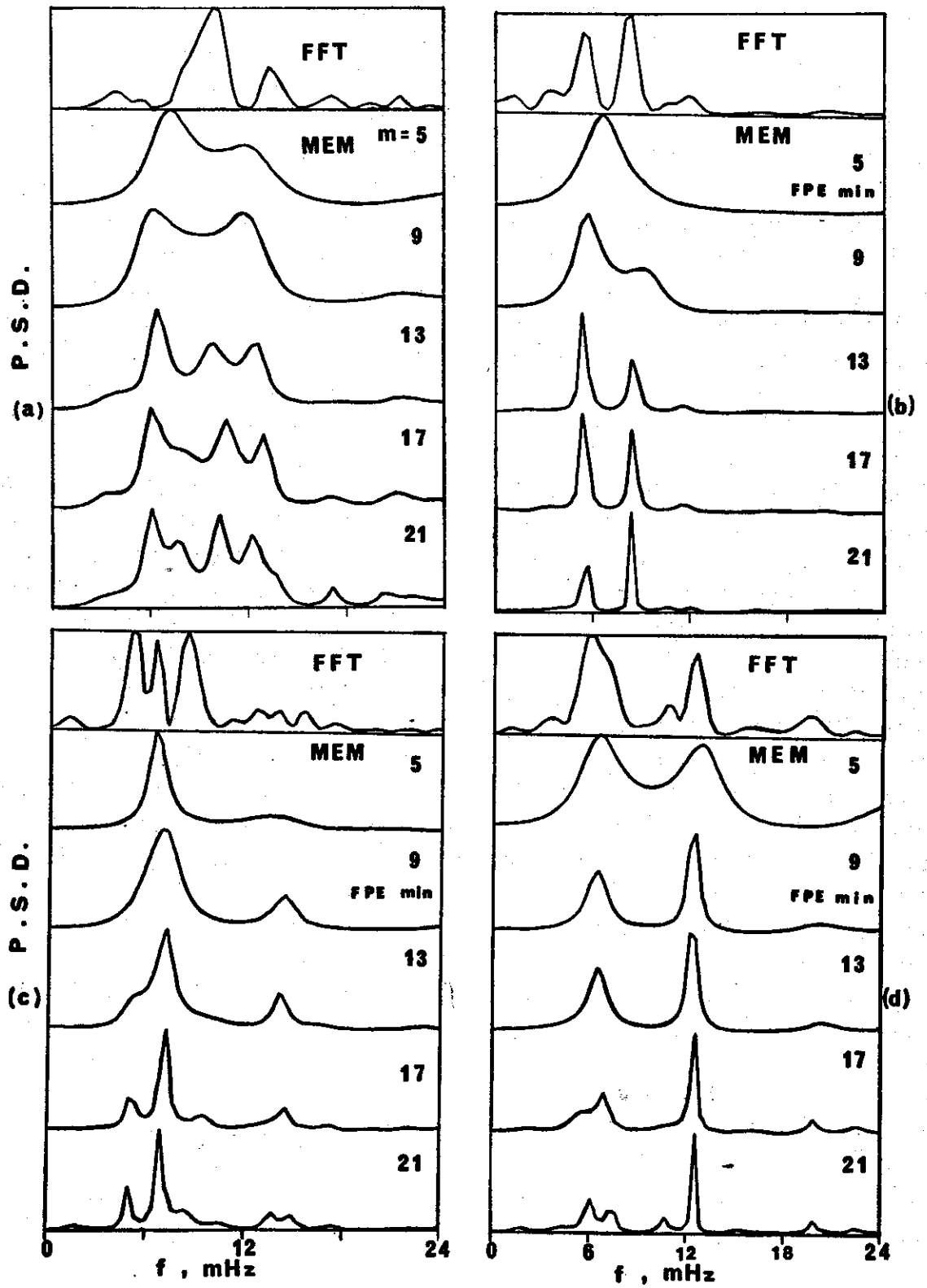

Figure 8. FFT and MEM spectra for 4 different 64-point sequences of Pi2 micropulsation data (see text for details).

stability of the estimates for various orders is fairly good especially when there is one predominant peak in the spectrum. This is illustrated in Figure 9 where spectra from 4 different short data samples are shown. The first spectrum from top is the FFT and the rest are MEM spectra for orders ranging from $m = 2$ to $m = 6$. The latter are relatively stable and consistent especially when $m = 4$, 5, and $m = 6$. The results from a large number of short data segments suggest that m should be at least equal to N/2. The superiority of MEM, as compared to the periodogram method, in terms of frequency resolution is clearly illustrated in Figure 9. However, even for short sequences, the MEM estimate for a particular order can be in doubt. Our experience shows that the stability of the MEM spectrum for different orders m depends on the particular data sample under analysis. It was found that in a limited number of short sequences, there is variability in the MEM spectrum even for successive orders. This is most likely to occur when there are two or more spectral peaks in a short data sample.

5. CONCLUDING REMARKS

The primary purpose of this paper was to compare the results of the conventional periodogram and of the maximum entropy method of spectral analysis on synthetic and real data in order to evaluate the performance of those two spectral techniques.

The periodogram, as expected, gave good spectral estimates for long data samples; the main problem is the poor frequency resolution for short data segments. The results of MEM were found in general to be superior in terms of frequency resolution, as has been pointed out by many others, but this does not mean necessarily that this method can lead to a completely accurate spectrum. The MEM exhibits different degrees of sensitivity for different spectral characteristics. For example, from experiments with harmonics plus noise it was found that in many cases the frequency location and spectral width of the peaks can be estimated accurately, but that the amplitude of the peaks may be in error. The latter can be a serious limitation of the technique and, to our knowledge, has not been given appropriate attention in the literature.

The choice of order of the AR process, which can be important especially for waveforms with complex spectrum, always involves a degree of uncertainty. The results suggest that the FPE criterion provides some guidance but not explicit solutions. It was found from experiments with relatively long synthetic data sequences that a substantial range of orders (from about $m = N/5$ to $2N/5$) exists that may yield a reasonably good spectrum. For such cases, it was suggested that a more stable MEM estimate may be obtained by averaging a number of spectra corresponding to different orders lying in the above range. Comparison of periodograms and MEM spectra for long segments of Pi2 data shows only general agreement and suggests that the FPE criterion underestimates the optimum order of the AR process that fits the data. For short sequences the FPE is of limited usefulness and an order at least equal to half the number of data points must be used.

The MEM performance depends on how well the AR process fits the available data. The goodness of fit, which can be influenced from unpredictable factors such as the noise level, the initial phase of the

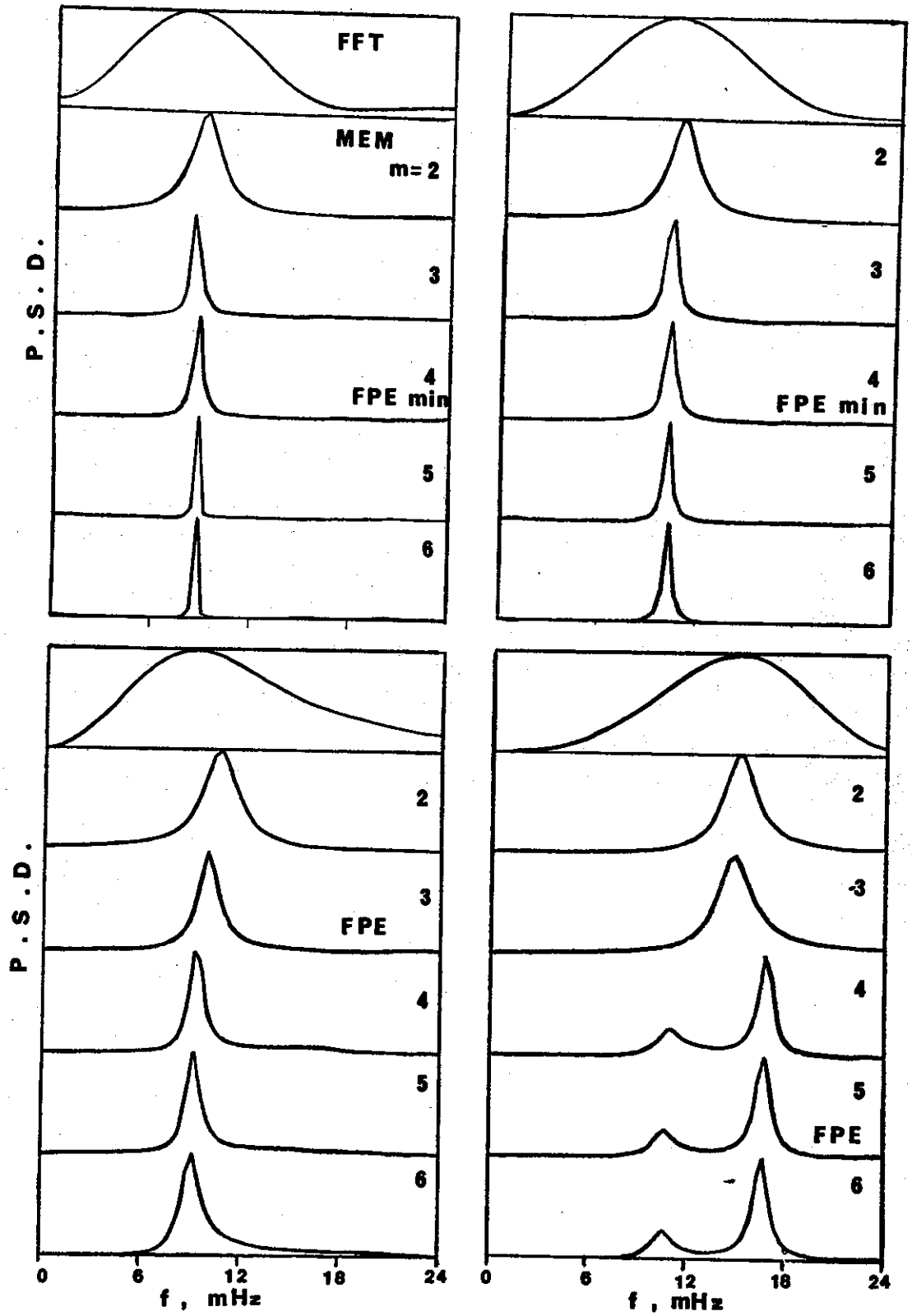

Figure 9. A series of FFT and MEM spectra for 4 different short 8-point (160 s) samples of Pi2 micropulsation data. The stability of the MEM estimates for different orders supports the reliability of the spectrum. These examples emphasize the superior frequency resolution of MEM spectrum over the periodogram for short data segments.

harmonics, and the compexity of the spectrum, depends on the particular data segment under analysis. Therefore, in view of the inherent limitations of MEM which emerge from the fact that it is strongly data dependent, this technique must be used with care. In any case, there is no strong reason why it is to be preferred to the periodogram, at least for long sequences. For short sequences, the performance of MEM is more successful and this technique can yield a good spectral estimate for most of the cases, but not always. Even for short sequences, there are factors (e.g. selection of optimum order, length of sequence, complexity of spectrum) which can lead to a false spectrum. However, overall it can be stated that the MEM is preferable to the periodogram method when one deals with limited data segments.

ACKNOWLEDGEMENTS

I wish to thank Prof. Alv Egeland of the Institute of Physics, University of Oslo, for his support and encouragement in this work. Financial assistance was provided by the Royal Norwegian Council for Scientific and Industrial Research (NTNF) in the form of a postdoctorate fellowship.

REFERENCES

Akaike, H. 1969. *Ann. Inst. Stat. Math. 21*, 407.

Alam, A. M. 1977. Adaptivē spectral estimation, Joint Autom. Control Conf. Vol. 1., June 22–24, p. 105.

Andersen, N. 1974. *Geophys. 39*, 62.

Blackman, R. B. & Tukey, J. W. 1958. P. 14 in *The Measurement of Power Spectra*. Dover Publications. New York.

Bringham, C. Godfrey, M.D. & Tukey, J. W. 1967. IEEE Trans. Audio and Electroacoust. *AU–15*, 56.

Burg, J. P. 1967. Maximum entropy spectral analysis, paper presented at the 37th Annual International Meeting, Soc. of Explor. Geophysicists.

Chen, W. Y. & Stegen, G. R. 1974. *J. Geophys. Res. 79*, 3019.

Childers, D. G. 1978. p. 1 in *Modern Spectrum Analysis*. Ed. D. G. Childers. IEEE Press. New York.

Fougere, P. F. 1977. *J. Geophys. Res. 82*, 1051.

Haldoupis, C. I. 1980. Institute of Physics, University of Oslo. Report 80–04.

Landers, T. E. & Lacoss, R. T. 1977. IEEE Trans. Geosci. Electron. *GE-15*, 26.

Otnes, R. K. & Enochson, L. 1978. p. 414 in *Applied Time Series Analysis*, John Wiley and Sons. New York.

Parzen, E. 1974. IEEE Trans. Automat. Control. *AC-19*, 720.

Ulrych, T. J. & Bishop, T. N. 1975. *Rev. Geophys. 13*, 183.

Van den Bos, A. 1971. IEEE Trans. Inf. Theory. *IT-17*, 493.

Instructions to Authors

GEOPHYSICA NORVEGICA

publishes papers in English. When preparing manuscripts for submission, authors should consult current copies of the journal and follow its style as closely as possible.

MANUSCRIPTS

Manuscript must be typewritten, double spaced throughout, on one side of the paper, with a wide margin. Authors should submit the *original* manuscript (preferably with one copy) to the editor, whose address is shown on page 2 of the cover.

Separate sheets should be used for the following: 1) title page, with the author's name and institution, and, if the title is longer than 40 letters and spaces, a short title not exceeding this limit for use in the running heads; 2) an abstract not exceeding 12 lines (910 letters and spaces) with the name and full postal address underneath of the author to whom communications, proofs, and reprints are to be sent; 3) references; 4) Tables with their headings; 5) legends to Figures.

Brief *Acknowledgements* of grants and other assist ance, if any, will be printed at the end of the text.

FIGURES, TABLES AND MATHEMATICAL SYMBOLS

All illustrations are to be considered as Figures. Each graph, drawing, or photograph should be numbered in sequence with arabic numerals, and should be identified on the back by the name of the journal, the author's name, and the Figure number. The top should be indicated. The Figures should be the original drawing. The columns of *Geophysica Norvegica* are 67 mm broad, and the size of the original drawings should be in proportion. Lines must be thick enough to allow for reduction. Letters and numbers should not be less than 2 mm high in the printed illustration. Photographs should be submitted as unmounted glossy enlargements showing good details.

Tables are to be numbered consecutively. Each Table should be typed on a separate sheet, with a descriptive heading that makes the Table self-explanatory.

All Figures and Tables should be referred to in the text by their number. Their approximate position should be indicated in the margin of the manuscript.

All numbered equations and all unnumbered but complicated equations should be typed on separate lines. Equations should be punctuated.

All text material will be set in roman type unless otherwise marked. Hence, all variables and other characters to be set in italic type should be underlined once with a straight line. Vectors and other characters in boldface type should be indicated by underlining with a single wavy line.

No footnotes should be used.

REFERENCES TO LITERATURE

In the text, Brown (1957, p. 9), Brown & White (1961). If more than two authors, Brown et al. (1963). Multiple references: 'As several authors have reported (Brown 1967, Brown & White 1961, Green et al. 1963)', i.e. chronological order, no commas between names and year.

Lists of References are to be unnumbered and in alphabetical order. The international alphabetical order of Scandinavian and German vowels should be observed: Å = AA, Æ and Ä = AE, Ø and Ö = OE, Ü = UE. Indicate 1st, 2nd, 3rd, etc. works by the same author in the same year by a, b, c, etc. (White 1966a). No ditto marks should be used. Titles of journals should be abbreviated according to *World List of Scientific Periodicals.*

Examples:

Cadle, R. D. 1966. p. 83 in *Particles in the Atmosphere and Space.* Reinhold Publishing Corporation, New York.

Craig, R. A. 1965. p. 161 in *The Upper Atmosphere. Meteorology and Physics.* International Geophysics Series, Vol. 8. Academic Press, New York and London.

Eliassen, A. & Kleinschmidt, E. 1957. p. 66 in *Handbuch der Physik.* Vol. 48, Part 2, edited by S. Flügge. Springer-Verlag, Berlin.

Junge, C. 1972. *Quart. J. R. Met. Soc. 98,* 711.

PROOFS

Two copies of the first proof will be sent (page proofs). One copy, duly corrected, should be returned to the editor with the least possible delay. All technical parts of the article, including references, names, figures (numbers, formulae), illustrations, etc. are the responsibility of the authors. Authors will be required to pay for any major alterations they may make.

REPRINTS

Fifty reprints of each article will be supplied free. Additional reprints can be ordered at a charge.